

51-25
137134
N93-15387²³⁰

Theoretical Characterization of the Potential Energy Surface
for NH + NO

Stephen P. Walch^a
ELORET Institute
Palo Alto, Ca. 94303

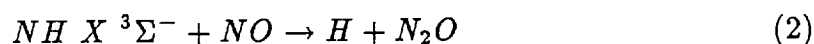
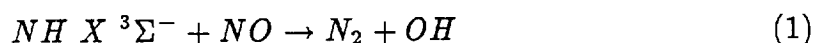
Abstract. The potential energy surface (PES) for NH + NO has been characterized using complete active space self-consistent field (CASSCF) gradient calculations to determine the stationary point geometries and frequencies followed by CASSCF/internally contracted configuration interaction (CCI) calculations to refine the energetics. The present results are in qualitative accord with the BAC-MP4 calculations of Melius and Binkley, but there are differences as large as 8 kcal/mol in the detailed energetics. Addition of NH to NO on a $^2A'$ surface, which correlates with $N_2 + OH$ or $H + N_2O$ products, involves barriers of 3.2 kcal/mol (trans) and 6.3 kcal/mol (cis). Experimental evidence for these barriers is found in the work of Böhmer et al. The $^2A''$ surface has no barrier to addition, but does not correlate with products. Surface crossings between the barrierless $^2A''$ surface and the $^2A'$ surface may be important. Production of $N_2 + OH$ products is predicted to occur via a planar saddle point of $^2A'$ symmetry. This is in accord with the preferential formation of $\Pi(A')$ Λ doublet levels of OH in the experiments of Patel-Misra and Dagdigian. Addition of NH $^1\Delta$ to NO is found to occur on an excited state surface and is predicted to lead to N_2O product as observed by Yamasaki et al.

^aMailing Address: NASA Ames Research Center, Moffett Field, CA 94035.

I. Introduction

The reaction of NH with NO is important in the combustion of nitrogen containing fuels and in the thermal De-NO_x process in which NO is converted to N₂ by the addition of NH₃ [1-4]. The latter process is important in controlling NO_x emissions from jet engines.

Considering the X ³Σ⁻ ground state of NH, there are two exothermic product channels.



Experimental estimates of the product branching ratio vary widely. Yamasaki et al. [5] concluded that reaction (1) accounted for 100 % of the products, while Mertens et al. [6] reported that reaction (1) accounted for only 19 ± 10 % of the products.

The PES for reaction (1) [7,8,9] involves an intermediate HNNO complex which undergoes a 1,3-hydrogen shift with a barrier to form an NNOH species which is unstable and dissociates to N₂ + OH. The HNNO complex can also dissociate over a barrier to H + NNO. The reverse process

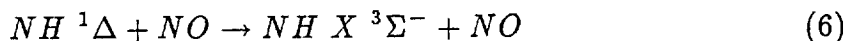


has also been studied. Reaction (3) can occur via a direct process in which H attaches to the O end of N₂O, or via an indirect process in which the H attaches to the end N of N₂O and then undergoes a 1,3-hydrogen shift leading to products via the same saddle point as for reaction (1) [8].

The internal energy distribution of the OH product for reaction (1) has been studied by Patel-Misra and Dagdigian [10] in a crossed beam experiment. The OH $v=1$ to $v=0$ vibrational population ratio was found to be 0.30 ± 0.06 and the average rotational energy was found to be 25 ± 1 kJ/mol (5.97 ± 0.23 kcal/mol). These authors note that this is a rather small amount of internal excitation given that reaction (1) is exothermic by 408 kJ/mol (97.5 kcal/mol). Attempts to model the internal energy distribution in the OH product by phase space theory lead to more excitation than observed, suggesting that the HNNO complex may not be long enough lived to exhibit statistical behaviour. In this study the internal energy distribution in the N_2 was not measured and it was presumed that most of the excess energy went into relative translational energy of the products. More recently, Böhmer et al. [11] have studied the reaction of N_2O with hot H atoms formed by photolysis of an N_2O -HI complex. This study is in general agreement with the work of Patel-Misra and Dagdigian with respect to the OH internal energy distribution, but the OH Doppler shift profiles in these experiments require a large amount of internal vibrational excitation of the N_2 ($\approx 25,000$ cm^{-1} (71.5 kcal/mol) for OH $v=0$). This result is explained by a model in which the HNNO complex has an elongated NN bond and the 1,3-hydrogen shift is assumed to occur rapidly with respect to motion of the heavy atoms leaving the N_2 product vibrationally excited. A more detailed understanding of the product energy distributions and branching ratios in this system requires more detailed information about the PES, which is reported in this paper.

Unlike many other reactions of NH, where the $^1\Delta$ state is more reactive, the NH + NO reaction is found to have comparable rates for the ground $X^3\Sigma^-$ state and the low lying $^1\Delta$ state of NH [5]. Yamasaki et al. [5] find a strong product specificity depending on the NH spin state. The ground state of NH leads to $N_2 + OH$ as the

predominant product, while the $^1\Delta$ state of NH also leads to $H + N_2O$. In addition, NO is able to quench NH $^1\Delta$ to NH $^3\Sigma^-$.



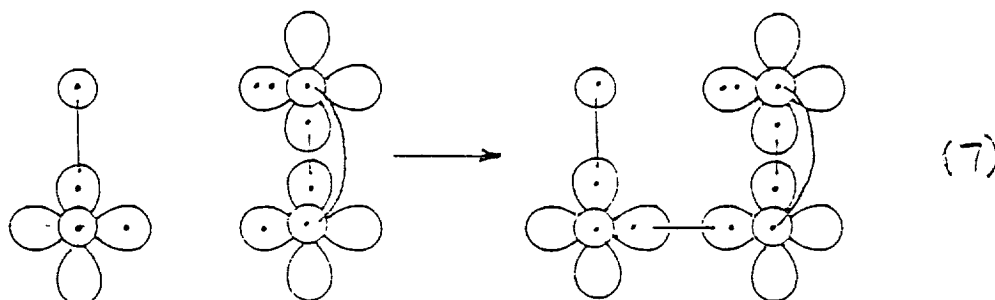
In the work of Yamasaki et al. the experimental results are analyzed in terms of a model based on a calculated PES by Melius and Binkley [7] and Fueno et al. [9]. In this picture NH ($^1\Delta$) + NO correlates with a $^2A'$ surface which also correlates with $H + N_2O$, while NH ($X\ ^3\Sigma^-$) + NO correlates with a HNNO complex on the $^2A''$ surface. As discussed below, this model is substantially oversimplified. In fact NO + NH in the $^3\Sigma^-$ and $^1\Delta$ state lead to six surfaces which are strongly coupled and the reaction of the $^1\Delta$ state of NH is a carbene insertion process which occurs on an excited state surface. Preliminary calculations on the excited state surfaces are also reported here.

There have been several previous studies of the PES for NH + NO. The most extensive of these is by Melius and Binkley [7] and used the BAC-MP4 method with a 6-31G** basis set. More recently Fueno et al.[9] have also carried out multi reference configuration interaction (MRCI) studies of this system using smaller basis sets. The present calculations are similar in spirit to these earlier studies, but use larger basis sets and more extensive configuration interaction. Thus, the present results are expected to be more reliable than the earlier studies. Qualitative features of the potential energy surfaces are discussed in Sec. II, the computational method is discussed in Sec. III, the results are presented in Sec. IV, and the conclusions are given in Sec. V.

II. Qualitative Features.

Combining the $^3\Sigma^-$ ground state of NH with the $^2\Pi$ ground state of NO and keeping a plane of symmetry leads to $^2,^4A'$ and $^2,^4A''$ surfaces. (It should be noted here that for four atoms the reaction may occur without symmetry; however, the key stationary points on the surface are found to have C_s symmetry and this symmetry is assumed in the following discussion.)

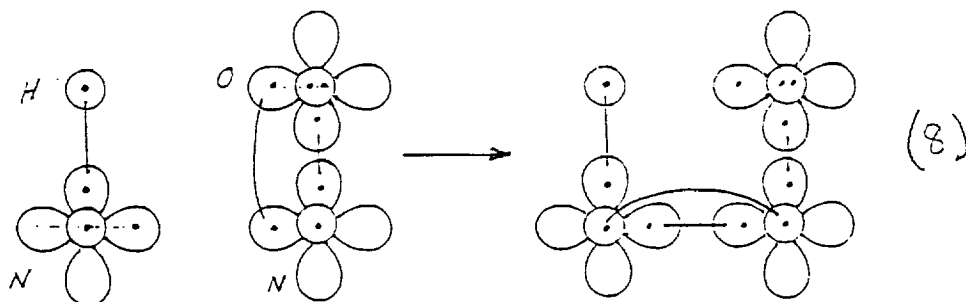
For the $^2A''$ surface, the singly occupied NO 2π orbital is in the plane of the supermolecule and addition of NH to NO occurs with no barrier.



However, a doubly occupied O $2p$ orbital is in the plane of the supermolecule and 1,3-hydrogen migration is unfavorable. Thus, approach on this surface would not be expected to lead to $N_2 + OH$ products. Also this surface can not lead to $H + N_2O$, since this product channel is of $^2A'$ symmetry.

For the $^2A'$ surface, the singly occupied NO 2π orbital is perpendicular to the plane of the supermolecule and the NH is adding to an NO π bond. Thus, a barrier to addition is expected on this surface. However, a singly occupied O $2p$ orbital is in the plane of the supermolecule and 1,3-hydrogen migration leading to NNOH may occur. This process is expected to have a barrier since an NH bond is being broken as the OH bond is formed. The NNOH species is not bound and the 1,3-hydrogen migration leads directly to $N_2 + OH$.

Fig. 1 shows a schematic of the potential energy surface for NH + NO. Focusing

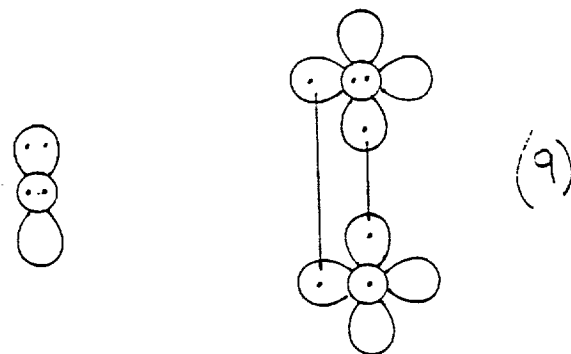


first on the features discussed above, it is seen that $\text{NH} + \text{NO}$ may form HNNO in the cis or trans orientation with no barrier on the ${}^2A''$ surface, but there are barriers on the ${}^2A'$ surface. HNNO corresponds to a stable planar minimum on the PES and the ${}^2A'$ state is lower than the ${}^2A''$ state. This leads to entrance channel surface crossings between these two surfaces, which may lead to surface hopping between the ${}^2A''$ surface, which forms with no barrier, and the ${}^2A'$ surface, which has an entrance channel barrier but leads to products. cis- HNNO on the ${}^2A'$ surface may undergo a 1,3-hydrogen shift leading to $\text{N}_2 + \text{OH}$ products.

From Fig. 1 it is also seen that $\text{H} + \text{NNO}$ correlates with the ${}^2A'$ surface. Addition of H to the O end of N_2O leads directly to $\text{N}_2 + \text{OH}$ with a large barrier. An alternative indirect pathway involves addition of H to the end N of N_2O which leads to cis- HNNO with a smaller barrier than addition to the O end. This pathway then connects to $\text{N}_2 + \text{OH}$ by the same 1,3-hydrogen shift saddle point involved in the $\text{NH} + \text{NO}$ reaction. The indirect pathway has a lower overall barrier and should be the predominate pathway at lower temperatures.

Addition of the low-lying ${}^1\Delta$ excited state of NH to NO involves a geometry in which the N atom of NH approaches near the midpoint of the NO bond with the NH bond approximately perpendicular to the plane formed by the N atom of NH and the NO bond. Combining the ${}^3\Sigma^-$ and ${}^1\Delta$ states of NH with the ${}^2\Pi$ state of

NO leads to six potential energy surfaces. Of these the lowest two are the ${}^2A'$ and ${}^2A''$ surfaces which correlate with the ${}^3\Sigma^-$ ground state of NH. Of the remaining four surfaces three are repulsive and one is attractive. The electronic configuration of the attractive state is:



(where the doubly occupied N 2p orbital perpendicular to the plane represents the NH bond pair of NH) This configuration is analogous to the configuration involved in insertion of $O({}^1D)$ into H_2 [12]. This configuration can also correlate with $H + N_2O$, since dissociation of the NH bond leads to a configuration with four a' and four a'' (with respect to the NNO plane) electrons in π orbitals on the N_2O . It is probable that this excited surface accounts for the production of N_2O observed by Yamasaki et al. [5] in the reaction of $NH\ {}^1\Delta$ with NO.

III. Computational Details.

Two different basis sets were used in this work. For the CASSCF gradient calculations the polarized double zeta set of Dunning and Hay [13] was used. The basis set for N and O is a (9s5p)/[3s2p] basis augmented by a single set of 3d functions with exponents of 0.80 and 0.85 for N and O, respectively. The H basis is (4s)/[2s] augmented with a single set of 2p functions with exponent 1.00. The basis set used in the CI calculations is the Dunning correlation consistent triple zeta double polarization basis set [14]. This basis is [4s3p2d1f] for N and O and [3s2p1d] for H

and is described in detail in Ref. 14.

The CASSCF calculations had 13 electrons distributed among 8 a' and 3 a'' orbitals. The active electrons correspond to the electrons depicted in Eqns. 7 and 8 plus the 2s electron pair on the central N. The remaining 10 electrons are the two pairs of N 1s electrons, the O 1s and 2s electron pairs, and the N 2s electron pair on the end N. One N 2s pair has to be active to describe certain regions of the surface (e.g. $H + N_2O$) where the N 2s electrons on the central N are used in bonding.

All but the N 1s and O 1s electrons are correlated in the subsequent CCI calculations. A selected reference list was used with a coefficient cutoff of 0.04.

The CASSCF/gradient calculations used the SIRIUS/ABACUS system of programs [15], while the CCI calculations were carried out with MOLPRO [16,17]. Most of the calculations were carried out on the NASA Ames Cray Y-MP. Some of the CCI calculations were carried out on the NAS facility YMP.

IV. Discussion.

Before discussing the results for the $HN + NO$ reaction, it is useful to consider results for the molecular species involved. Table I compares geometries and harmonic vibrational frequencies from CASSCF/gradient calculations for NH, NO, N_2O , OH, and N_2 with experiment. The results shown in Table I are typical of results obtained at stable minimum points on a PES using CASSCF/gradient methods. Here it is seen that the bond lengths are too long by $\approx 0.02 \text{ \AA}$ but the vibrational frequencies are in fair agreement with experiment. This result contrasts with the results of Hartree-Fock theory, which typically gives bond lengths which are somewhat shorter than experiment and frequencies which are larger than experiment. It has been common practice to scale SCF frequencies by ≈ 0.9 to account for this defect in the SCF results. The CASSCF frequencies on the other hand are approximately correct and are used here without scaling.

Tables IIa and IIb show comparisons of CASSCF/gradient and externally contracted CI [18] calculations for the HN_2 and HO_2 surfaces. Once again at the minima on the PES's, corresponding to HN_2 and HO_2 , the geometries and frequencies are in fair agreement with the more accurate CCI results. (The bond lengths from the CASSCF calculations are slightly too long as noted above.) At the saddle points the CASSCF results are poorer. In both cases the saddle point geometry is tighter in the CASSCF calculations than in the CCI calculations, as evidenced by a shorter HN/HO bond length, a larger bending frequency, and a larger imaginary frequency at the saddle point. It is also seen from Table II that the binding energies are smaller in the CASSCF calculations. These results are typical, based on experience with other systems. For HN_2 it has been shown that addition of a correction term, which is a slowly varying function of the NH bond length, to the CASSCF surface results in a reasonable approximation to the CCI surface [19]. This result suggests that the CASSCF surface is mainly distorted along the reaction coordinate, but is a better representation in the directions orthogonal to the reaction coordinate. Thus, one way to correct the CASSCF surface near a saddle point would be to compute CI energies along the minimum energy path on the CASSCF surface. This approach has actually been carried out for the reaction of $^1\text{CH}_2 + \text{H}_2\text{O}$ [20], which is a barrierless process. However, for the present system the saddle points involve barriers and are expected to be less sensitive to small changes of the geometry along the reaction coordinate. Thus, the approach used here is to carry out CCI calculations at the stationary point geometries obtained at the CASSCF level.

Tables IIIa and IIIb give computed frequencies and geometries for the $^2\text{A}'$ and $^2\text{A}''$ states of HNNO , respectively. Table IV gives the computed CCI energies at each of the stationary points, the zero-point energies, and the relative energies (

including zero-point energy). The same energetics are shown graphically in Fig. 1.

From Table IIIa it is seen that addition of NH to NO on the $^2A'$ surface occurs with loose saddle points i.e. the bond lengths and frequencies are close to those for NH and NO. The saddle points for adding H to the end N and O of N_2O show somewhat more distortion of bond lengths, r_{NN} elongated by 0.03 Å for H-NNO and r_{NO} elongated by 0.07 Å for NNO-H.

Cis and trans HNNO on the $^2A'$ surface have similar bond lengths. Both the NN and NO bond lengths of HNNO on the $^2A'$ surface are shorter than on the $^2A''$ surface. The NN bond length is shorter by 0.10 Å and 0.12 Å for cis and trans HNNO, respectively. This effect results from the greater NN π bonding on the $^2A'$ surface which is evident from Eqn's (7) and (8). The shorter NO bond on the $^2A'$ surface is probably due to smaller non-bonded repulsions between the doubly occupied O 2p orbital and the NN bond orbitals.

The saddle point for 1,3-hydrogen migration in cis-HNNO leading to $N_2 + OH$ product (denoted NNOH in Table IIIa), by contrast with the other saddle points discussed above, would be described as a tight saddle point. Here the NN bond is elongated by 0.11 Å (compared to a comparable N_2 calculation, Table I). As discussed by Böhmer et al. [11] (see section I), this elongation of the NN bond is believed to be responsible for the production of vibrationally excited N_2 product.

Table V compares the geometries and frequencies obtained in the present calculations with the BAC-MP4 results of Melius and Binkley [7,21]. It should be noted that the frequencies reported by Melius and Binkley have been scaled downward by 12 %. For cis-HNNO the CAS bond lengths are somewhat longer than those obtained with the BAC-MP4 method. This is expected from the discussion above. The frequencies are in fair accord but there appears to be a tendency for the CAS frequencies to be larger than the scaled UHF frequencies. For the saddle points the

CASSCF geometries are again in reasonable accord with the UHF geometries (taking into account the tendency for CAS to slightly overestimate bond lengths). One interesting difference is that CAS leads to a larger imaginary frequency for NNO-H compared to NNOH, while UHF shows the opposite trend. This could have some significant dynamical consequences, because in Ref. 8 a one dimensional tunneling correction was made based on the imaginary frequency.

Table VI compares the CAS/CCI energetics with those obtained using the BAC-MP4 method. Here there is sporadic agreement. In particular, the NNO-H and NNOH saddle point energies agree to within 2 kcal/mol with the present calculations, but the H-NNO saddle point is 6.7 kcal/mol lower in the present calculations. A peculiar result is that the BAC-MP4 calculations find cis-HNNO below trans-HNNO which is the opposite of what is found in the present calculations. It should be noted here that the BAC-MP4 method makes rather large corrections (≈ 10 kcal/mol for single bonds and ≈ 20 kcal/mol for double bonds) to the energies. The present calculations use no empirical corrections yet yield results of at least as good accuracy. The incorrect ordering for cis and trans HNNO is puzzling because the correct ordering is obtained with CASSCF and CCI. Still the present results tend to support the utility of the BAC-MP4 method, though the present large scale CI calculations are undoubtedly more reliable.

We now turn to a more detailed discussion of the computed potential energy surface as shown in Fig. 1 and based on the energetics given in Table IV. As shown in Fig. 1 there are barriers to the addition of NH to NO on the $^2A'$ surface. The computed barrier heights are 6.3 kcal/mol for cis approach and 3.2 kcal/mol for trans approach. These barriers are expected based on the discussion in Section II and are similar in origin to barriers for addition of H to NO [22]. Experimental verification of these barriers is obtained in experiments of Böhmer et al. [11] which

measure the threshold for formation of $\text{NH } ^3\Sigma^-$ in the reaction of hot H atoms with NO formed by photolysis of an HI-NO complex. These experiments indicate a threshold occurring for a photolysis wavelength between 250 and 260 nm whereas the energy of the lowest vibrational level of $\text{NH } ^3\Sigma^- + \text{NO}$ occurs at ≈ 270 nm, a difference of $\approx 4\text{-}9$ kcal/mol. It should be noted here that $\text{H} + \text{NO}$ correlates with the $^2\text{A}'$ surface and dissociation to $\text{NH} + \text{NO}$ therefore should involve a barrier.

Addition on the $^2\text{A}''$ surface involves no barrier but this surface does not correlate with $\text{H} + \text{N}_2\text{O}$ nor, from the discussion in Section II, is it likely to lead to $\text{OH} + \text{N}_2$ products. Because the $^2\text{A}'$ surface drops more rapidly than the $^2\text{A}''$ surface, surface crossings are expected in the $\text{NH} + \text{NO}$ entrance channel region. These surface crossings may allow addition to occur on the barrierless $^2\text{A}''$ surface with subsequent surface crossing to the $^2\text{A}'$ surface which connects to products. This process could reconcile the apparent lack of a barrier to reaction (1) with the expectation that the products pass through the planar NNOH saddle point, which has $^2\text{A}'$ symmetry. Evidence that the products arise via a saddle point of $^2\text{A}'$ symmetry comes from the experiments of Petel-Misra and Dagdigian [10] in which a marked preference for $\Pi(\text{A}')$ Λ doublet levels is observed in the OH product.

The reverse reaction of $\text{H} + \text{N}_2\text{O}$ i.e reactions (3) and (4) has been studied by Marshall et al. [8] and by Böhmer et al. [11]. The present results are consistent with the discussion in Ref. 8. The production of $\text{N}_2 + \text{OH}$ can proceed via a direct process in which the H adds to the O end of N_2O . The computed barrier height for the direct pathway is 18.0 kcal/mol. The indirect pathway involves addition of H to the end N of N_2O which has a 10.3 kcal/mol barrier and a subsequent 1,3-hydrogen shift to yield products via the NNOH saddle point which has a 16.3 kcal/mol barrier. Thus, the indirect pathway has a lower overall barrier and should be the more favorable process at lower temperatures.

The reaction of the $^1\Delta$ excited state of NH with NO, reaction (5), has also been studied. The reaction of NH $^1\Delta$ with H_2 has been studied by Fueno et al. [23]. These authors observed an initial approach geometry in which the N atom approaches perpendicular to the midpoint of the H_2 bond and the NH bond is perpendicular to the plane formed by the N and H_2 molecule. Fig. 2 shows the electronic structure for the lowest six surfaces of NH + NO for this geometric arrangement. Two of these surfaces arise from the $^3\Sigma^-$ state of NH and the remaining four surfaces arise from the $^1\Delta$ state of NH. Of these surfaces the one which allows insertion is given by Eqn. (9). A limited study of this insertion process was made using a state averaged CASSCF calculation (averaged over the six lowest roots) varying only the N to NO bond midpoint distance (R) as shown in Fig. 3. From Fig. 3 curve crossings are evident between the diabatic states arising from NH $^3\Sigma^-$ state (repulsive) and the diabatic state arising from Eqn (9). If the H atom is allowed to dissociate from the initially formed HN-NO adduct, there are four electrons of π' and four electrons of π'' symmetry with respect to the NNO plane. Thus, this structure does correlate with the ground state of N_2O and it is plausible that production of N_2O via addition of NH $^1\Delta$ to NO occurs via the third excited surface.

V. Conclusions.

The potential energy surface for NH + NO has been characterized using CASSCF gradient calculations to determine the stationary point geometries and frequencies followed by CASSCF/ internally contracted CI calculations to determine the energetics. The CASSCF method is found to give reasonable geometries and frequencies at minima on the PES. At saddle points the geometries and frequencies are somewhat less accurate as revealed by comparison of CASSCF and CCI results for the HN_2 and HO_2 PES's. Studies of the HN_2 PES indicate that the CASSCF surface is distorted from the more accurate CCI surface mainly in the direction of the re-

action coordinate, while directions orthogonal to the reaction coordinate are better represented.

In general the present results are in qualitative accord with the work of Melius and Binkley using the BAC-MP4 method. However, the present calculations have no empirical corrections while the BAC-MP4 method involves large corrections (≈ 10 kcal/mol for single bonds and ≈ 20 kcal/mol for multiple bonds). There are also some large discrepancies (as large as 8 kcal/mol) in detailed energetics between the present work and the BAC-MP4 results.

Addition of NH to NO on a $^2A''$ surface involves barriers of 3.2 kcal/mol for trans orientation and 6.3 kcal/mol for cis orientation. The presence of these barriers is predicted from simple qualitative considerations and is supported experimentally by threshold measurements for production of NH + NO in the reaction of hot H atoms formed by photolysis of an HI-NO complex in the experiments of Böhmer et al.

Production of $N_2 + OH$ products is predicted to occur via a 1,3-hydrogen shift from an initially formed cis HNNO adduct of planar $^2A'$ symmetry. This conclusion is supported by experiments of Petel-Misra and Dagdigian in which a marked preference for $\Pi(A')$ Λ doublet levels is observed in the OH product.

Addition of NH $^1\Delta$ to NO is shown to occur on an excited state surface and to involve a geometry in which the NH approaches the NO with the N perpendicular to the NO bond midpoint and with the NH bond perpendicular to the NO-N plane. The electronic structure of this complex correlates with H plus the ground state of N_2O . This suggests that N_2O observed as the primary product in the reaction of NH $^1\Delta$ with NO by Yamasaki et al. occurs on this excited state surface.

ACKNOWLEDGMENTS

S.P. Walch was supported by a NASA grant(NCC2-478). The author thanks E.

Böhmer and P.J. Dagdigian for preprints of their work. Helpfull discussions with Carl Melius, Peter Taylor, and Curt Wittig are gratefully acknowledged.

References

1. J.A. Miller, M.C. Branch, and R.J. Kee, *Combust. Flame*, **43**, 81(1981).
2. R.K. Lyon, Sandia Laboratories Report No. SAND70-8635, 1970.
3. R.K. Lyon, U.S. Patent 3,900,544, August 1975.
4. R.K. Lyon, *Int. J. Chem. Kinet.*, **8**, 315(1976).
5. K. Yamasaki, S. Okada, M. Koshi, and H. Matsui, *J. Chem. Phys.*, **95**, 5087(1991).
6. J.D. Mertens, A.Y. Chang, R.K. Hanson, and C. Bowman, *Int. J. Chem. Kinet.*, **23**, 173(1991).
7. C.F. Melius and J.S. Binkley, In *Proceedings of the 20th Symposium (International) on Combustion*, The Combustion Institute: Pittsburg, Pa, 1984, p.575.
8. P. Marshall, A. Fontijn, and C.F. Melius, *J. Chem. Phys.*, **86**, 5540(1987).
9. T. Fueno, M. Fukuda, and K. Yokoyama, *Chem. Phys.* **124**, 265(1988).
10. D. Patel-Misra and P.J. Dagdigian, *J. Phys. Chem.*, **96**, 3232(1992).
11. E. Böhmer, S.K. Shin, Y. Chen, and C. Wittig, to be published
12. S.P. Walch and L.B. Harding, *J. Chem. Phys.*, **88**, 7653(1988).
13. T.H. Dunning, Jr and P.J. Hay in *Methods of Electronic Structure Theory*, H.F. Schaefer III ed., Plenum Publishing, 1977
14. Dunning ANO's
15. SIRIUS is an MCSCF program written by H.J. Jensen and H. Agren and ABACUS is an MCSCF derivatives program written by T. Helgaker, H.J. Jensen, P. Jørenson, J. Olsen, and P.R. Taylor.
16. H.-J. Werner and P.J. Knowles, *J. Chem. Phys.*, **89**, 5803(1988).

17. P.J. Knowles and H.-J. Werner, Chem. Phys. Lett., **145**, 514(1988).
18. P.E.M. Siegbahn, Int. J. Quantum Chem., **23**, 1869(1983).
19. S.P. Walch, unpublished results
20. S.P. Walch, to be published
21. C.F. Melius, private communication
22. S.P. Walch and C.M. Rohlfing, J. Chem. Phys., **91**, 2939(1989).
23. T. Fueno, V.B-Koutecky', and J. Koutecky', J. Am. Chem. Soc., **105**, 5547(1983).

Table I. Computed geometries and frequencies for fragments^a.

		calc.	exp.
NH	r_{NH}	1.062	1.038
	ω	3131	3282.09
NO	r_{NO}	1.174	1.1508
	ω	1889	1904.3
N ₂ O	r_{NN}	1.149	1.1282
	r_{NO}	1.204	1.1842
	ω_1	2267	2223.7
	ω_2	1297	1276.5
	ω_3	568(2)	589.2
OH	r_{OH}	0.988	0.9706
	ω	3624	3735.21
N ₂	r_{NN}	1.123	1.0977
	ω	2315	2358.027

^a bond lengths in Å and frequencies in cm⁻¹.

Table IIa. Comparison of CASSCF and CCI for HO₂^a

	H-O ₂		HO ₂	
	CAS/grad	CCI	CAS/grad	CCI
r _{OH}	3.55	4.14	1.86	1.84
r _{OO}	2.33	2.29	2.58	2.52
∠ HOO	116	116	102	104
ω ₁	596 <i>i</i>	412 <i>i</i>	3617	3531
ω ₂	1503	1515	1438	1417
ω ₃	501	354	1058	1220
E	1.9	0.4	-39.9	-51.2

^a Bond lengths in a₀, angles in degrees, frequencies in cm⁻¹, and E in kcal/mol.

Table IIb. Comparison of CASSCF and CCI for HN_2^c

	H-N ₂		HN ₂	
	CAS/grad	CCI	CAS/grad	CCI
r_{NH}	2.49	2.64	2.05	2.02
r_{NN}	2.19	2.17	2.27	2.25
$\angle \text{HNN}$	116	123	114	115
ω_1	1788 <i>i</i>	1387 <i>i</i>	2577	2577
ω_2	2004	2027	1735	1931
ω_3	892	668	1116	1106
E	27.4	15.8	23.6	5.6

^a Bond lengths in a_0 , angles in degrees, frequencies in cm^{-1} , and E in kcal/mol.

Table IIIa. Computed frequencies and geometries ($^2A'$ surface) ^a.

	HN+NO	cis HN-NO	trans HN-NO	H+N2O	H-NNO	cis HNNO
Γ_{NH}	1.06	1.06	1.06		1.47	1.05
Γ_{NN}		1.92	1.94	1.15	1.18	1.27
Γ_{NO}	1.17	1.18	1.18	1.20	1.21	1.23
\angle HNN		94.4	91.7		109.6	106.5
\angle NNO		117.3	120.0	180.0	160.2	134.8
ω_1	3131	3132	3190	2267	2033	3160
ω_2	1889	1738	1791	1297	1259	1630
ω_3		778	781	568	585	1373
ω_4		282	321	568	464	1201
ω_5		732 <i>i</i>	687 <i>i</i>		1724 <i>i</i>	549
ω_6		468	529		604	771
trans HNNO		NNO-H		NNOH		
Γ_{NH}	1.04	Γ_{OH}	1.41	Γ_{NH}	1.27	
Γ_{NN}	1.28	Γ_{NN}	1.16	Γ_{NN}	1.23	
Γ_{NO}	1.22	Γ_{NO}	1.27	Γ_{NO}	1.47	
\angle HNN	103.9	\angle HON	112.4	\angle HNN	1.38	
\angle NNO	129.6	\angle NNO	151.0	\angle NNO	89.9	
				\angle NOH	95.2	
				\angle OHN	76.7	
ω_1	3311		1989		98.1	
ω_2	1628		1132		2035	
ω_3	1382		860		1587	
ω_4	1228		474		890	
ω_5	589		2212 <i>i</i>		467	
ω_6	797		556		1934 <i>i</i>	
					948	

^a Bond lengths in Å, angles in degrees, frequencies in cm^{-1} .

Table IIIb. Computed frequencies and geometries ($^2A''$ surface) ^a.

	cis HNNO	trans HNNO
r_{NH}	1.06	1.05
r_{NN}	1.37	1.40
r_{NO}	1.27	1.25
$\angle HNN$	104.6	102.2
$\angle NNO$	111.8	109.1
ω_1	3188	3274
ω_2	1437	1464
ω_3	1233	1241
ω_4	736	741
ω_5	522	491
ω_6	550	394

^a Bond lengths in Å, angles in degrees, frequencies in cm^{-1} .

Table IV. Computed energies and zero-point corrections.

	Energy	zero-point energy	ΔE
NH+NO	-184.81050(-.85245)	0.01143	0.0
H+NNO	-184.85597(-.90221)	0.01071	-31.7
cis HN-NO	-184.78351(-.84556)	0.01457	6.3
trans HN-NO	-184.78893(-.85093)	0.01507	3.2
cis HNNO	-184.87106(-.93448)	0.01979	-46.2
trans HNNO	-184.87834(-.94352)	0.02036	-51.5
NNO-H	-184.80993(-.87431)	0.01142	-13.7
H-NNO	-184.82843(-.88698)	0.01189	-21.4
NNOH	-184.81960(-.87912)	0.01350	-15.4
cis HNNO $^2A''$	-184.83465(-.89268)	0.01746	-21.5
trans HNNO $^2A''$	-184.83635(-.89190)	0.01732	-21.1

Table V. Comparison of BAC-MP4 and CASSCF/CCI for NH + NO; Geometries and Frequencies^a

	cis HNNO		NNO-H		NNOH	
	CAS	UHF	CAS	UHF	CAS	UHF
r_{NH}	1.06	1.01	r_{OH}	1.41	r_{NH}	1.27
r_{NN}	1.27	1.23	r_{NN}	1.17	r_{NN}	1.23
r_{NO}	1.23	1.21	r_{NO}	1.27	r_{NO}	1.47
$\angle HNN$	106.5	109	$\angle HON$	112.4	r_{OH}	1.38
$\angle NNO$	134.8	132	$\angle NNO$	151.0	$\angle HNN$	89.9
ω_1	3160	3210	ω_1	1989	$\angle NNO$	95.2
ω_2	1630	1463	ω_2	1132	$\angle NOH$	76.7
ω_3	1373	1294	ω_3	860	$\angle OHN$	98.1
ω_4	1201	1042	ω_4	474	ω_1	2035
ω_5	549	312	ω_5	2212 <i>i</i>	ω_2	1587
ω_6	771	843	ω_6	556	ω_3	890
					ω_4	467
					ω_5	1934 <i>i</i>
					ω_6	948

^a Bond lengths in Å, angles in degrees, frequencies in cm⁻¹.

Table VI. Comparison of BAC-MP4 and CASSCF/CCI for NH + NO; Energetics

Stationary Point	BAC-MP4 ^{a,b}	CASSCF/CCI ^{a,c}
H + N ₂ O	0.0	0.0
NNO-H	19.8	18.0
H-NNO	3.6	10.3
[NNOH]	16.7	16.3
cis HNNO ² A'	-14.5	-14.5
trans HNNO ² A'	(-11.6)	-19.8

^a relative energy in kcal/mol.

^b 6-31G** basis set

^c [4s3p2d1f/3s2p1d] basis set

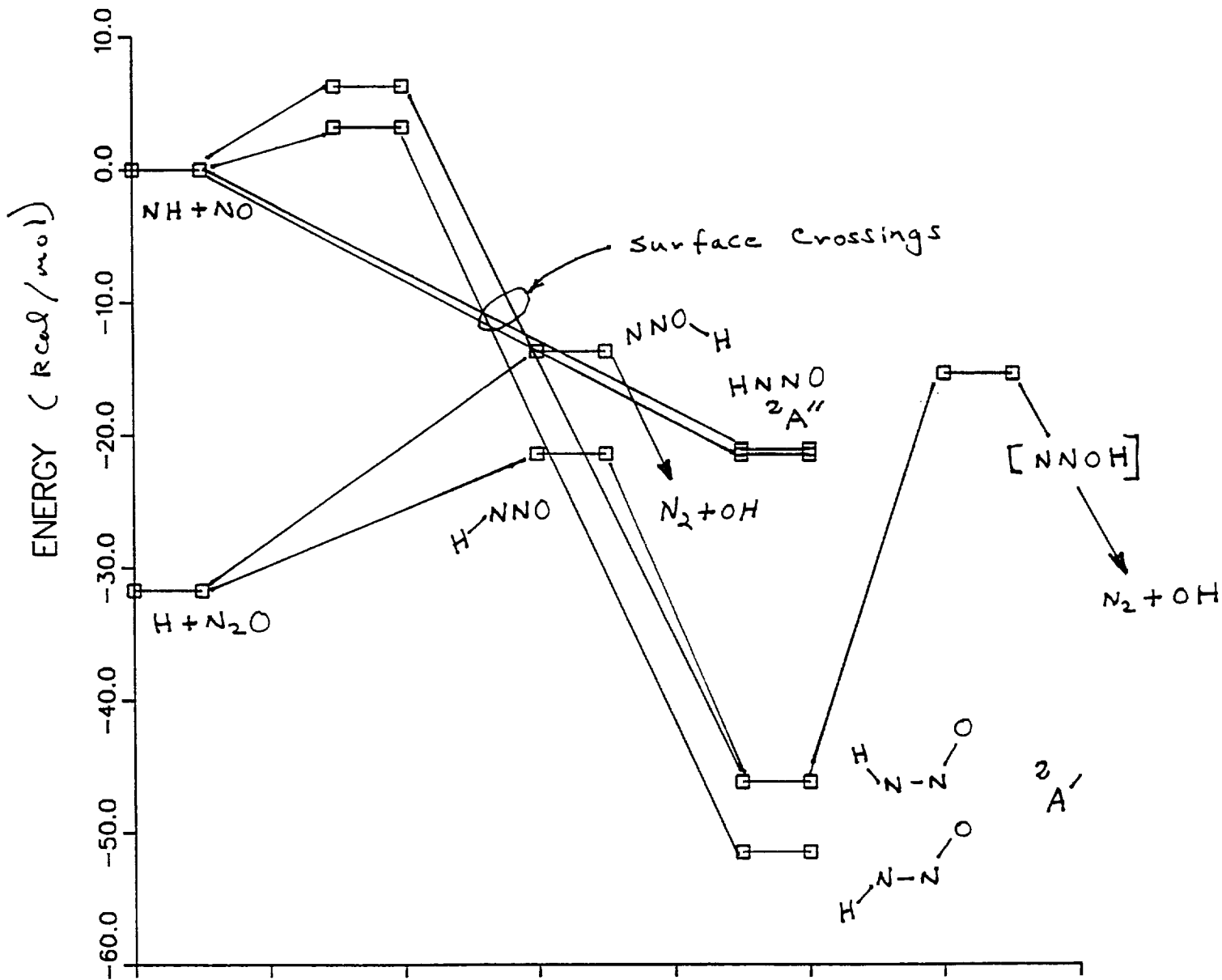
Figure Captions.

Fig. 1. Schematic of the potential energy surface for NH + NO. The stationary point geometries and vibrational frequencies are obtained at the CASSCF level, while the computed energetics are from CI calculations (See the text.). A region of crossing between $^2A'$ and $^2A''$ surfaces in the NH + NO entrance channel region is indicated.

Fig. 2. The asymptotic electronic structure of the six potential energy surfaces arising from NO $^2\Pi$ plus NH $^3\Sigma^-$ and NH $^1\Delta$.

Fig. 3. Potential energy curves for the lowest six potential energy surfaces for NH + NO as a function of R with the other geometrical parameters fixed (See the figure inset.).

Potential Energy Surface for NH + NO

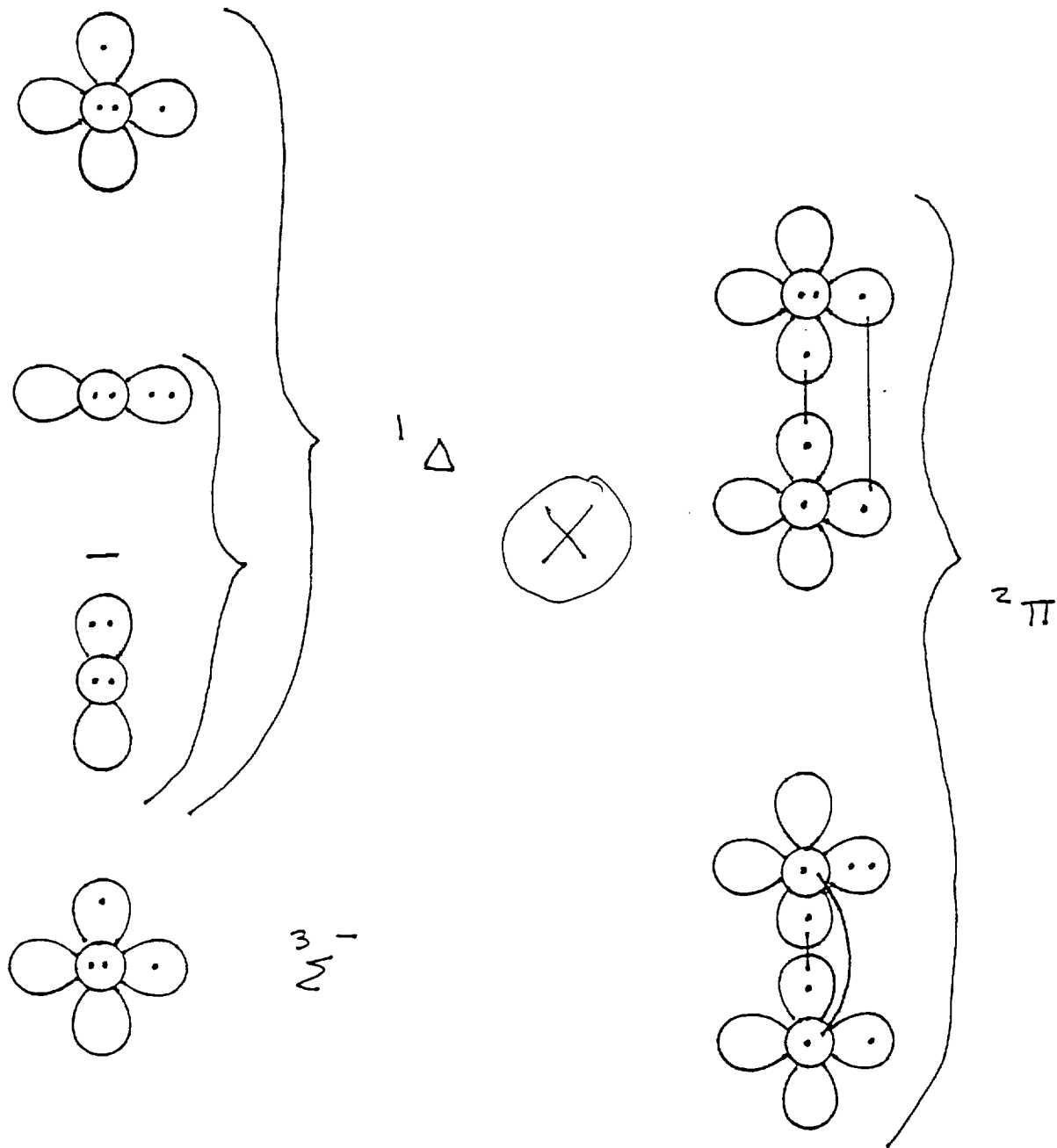


~~text~~

Fig. 2

13

NH + NO excited state surfaces



State averaged CASSCF results

